ARTICLE

Integrated analytical platforms for the comprehensive characterization of bioconjugated inorganic nanomaterials aiming at biological applications

Borja Moreira-Alvarez,[a] Laura Cid-Barrio,[a] Hadla S. Ferreira,[b] José M. Costa-Fernández *[a] and Jorge Ruiz Encinar *[a]

The synthesis of new multifunctional engineered nanoparticles (ENPs) constitutes nowadays a research topic of increasing importance in nano(bio)technology. Such ENPs can be synthesized out of a large variety of different materials, being inorganic nanoparticles highly competitive in biomedical applications due to their unique optoelectronic properties. Most bioapplications requires for their proper and controlled surface functionalization, which not only defines their interactions with the environment ultimately affecting their colloidal stability and biocompatibility, but also allows assembly of functional biomolecules capable to provide a controlled targeting and delivery of nanoparticles (mandatory for chemical sensing or bioimaging purposes). In this context, precise control of the composition and chemical quality of the starting nanomaterial is required as well to ensure their subsequent functionalization. This tutorial review is intended to provide a perspective on the different techniques that can be integrated into multidisciplinary analytical platforms for sizing, optical and elemental characterization of engineered structured inorganic nanomaterials before and after their bioconjugation to biomolecules.

1. Introduction

There are no doubts that nanoscience and nanotechnology have changed the pillars of the current research, being at present essential in a wide range of fields such as environment, food technology, cosmetic, medicine, chemistry, energy or material coating, to mention a few.[1] Such has been its relevance that it is considered the sixth technological revolution of the modern world.[2] Nanomaterials (NMi) can be defined as "natural, incidental or manufactured material containing particles, in an unbound state or as an aggregate or as an agglomerate and where, for 50 % or more of the particles in the number size distribution, one or more external dimensions is in the size range 1 nm - 100 nm; and it is considered as nanoparticle (NPs) if all its dimensions are in that range, regardless of whether its origin is natural or synthetic.[3] On this scale, the behaviour and physical-chemical properties of the nanomaterials are quite advantageous and very different from those of their macroscale equivalents. Notable among these are the large surface area to volume ratio (which may be orders of magnitude greater), conductivity and chemical reactivity, high electron density and strong optical absorption, intense and stable photoluminescence or magnetic moment. Some of these properties, which depend on the elementary composition, size[4] or surface chemistry;[5] make nanomaterial very attractive for their potential application in different biomedical applications including controlled drug delivery, photoablation therapy, bioimaging or biosensors.

In order to benefit from such exceptional features and exploit entirely the potential of NPs, it is necessary first to render them with biocompatibility and functionality using physico-chemical processes that often involve several reaction steps producing nanoassemblies sometimes with high compositional variability.[6] In that way, two or more individual entities (NPs, ligands, biomolecules) are so integrated in an engineered NMi that combines the properties of its individual components.[7] In the case of NMi, such chemical process usually implies the modification of their surface covering it with ligands, polymers and/or recognition elements to improve their solubility and affinity towards the biological target. Bioconjugation is the most critical step for the successful application of the NMi, due to the possibility of suffering different reactions when they enter into the target biological environment. These might range from surface modifications (e.g. oxidation) to undesirable unspecific interactions with other entities.[8] Therefore, it is necessary to carry out a previous complete characterization of the product resulting from the functionalization process in order to assess the quality of the bioassemblies and to find out if further purification is required and so ensure the successful application of the resulting NMi.

[a] Department of Physical and Analytical Chemistry, University of Oviedo, Julián Clavería, 8, 33006, Oviedo, Spain.
[b] Scholarship By CNPq, Brazil.
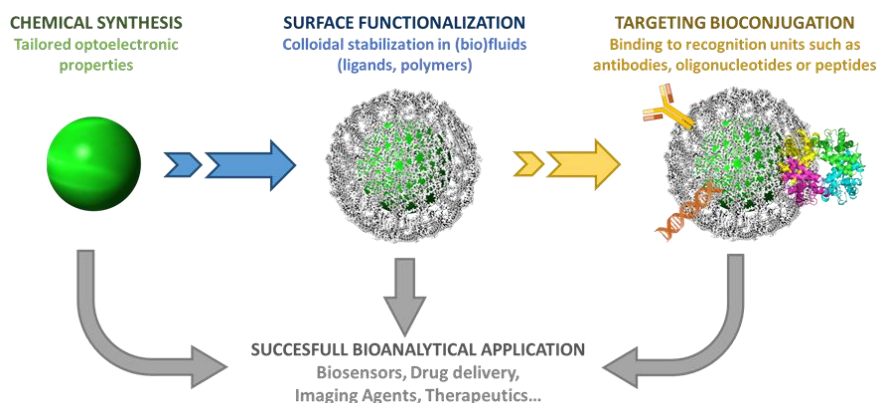* Corresponding authors: ruizjorge@uniovi.es; jcostafe@uniovi.es

Figure 1. General stages in the production of biocompatible and functionalized NMi. Comprehensive characterization of starting material, intermediates and final product is required in the development of successful applications.

On the other hand, the increased use of engineered NMi in many practical applications and their presence in daily consumer products have incited a global concern for their likely impact on the environment and their potential risk to our health and safety.[9] Since these adverse effects are also directly related to the synergistic effects of shape and surface functionalization of the nanoparticles, it is again required to develop analytical techniques for the comprehensive characterization of the new species finally resulting from the interactions of the engineered NMi with the matrix components present in the different media.[10,11]

To the best of our knowledge, there is currently no established method that allows the assessment of all those properties simultaneously. Usually, a range of different methods are used depending on the attribute to be studied.[12,13] Yet in spite of this complex multi-technique approach there are still certain parameters hard to characterize, such as purity or bioconjugate efficiency.[14] This work tries to gather together the different analytical approaches used to control and characterize the different steps and species formed along the functionalization process, from the originally synthetized NPs to the final engineered NMi (see Figure 1) and its potential modifications in the application media.

2. Inorganic nanoparticles

Among all types of NPs, metal-based particles have experienced a tremendous development for bioanalytical applications due to their small size, stability, optical properties, biocompatibility and great analytical sensitivity. As a matter of fact, traditional optical contrast agents used in bioanalytics are currently being replaced by photoluminescent NPs such as Nobel metal nanoclusters, quantum dots (QDs), carbon-based nanoparticles or rare earth NPs, due to their excellent optoelectronic properties, overcoming many of the limitations usually encountered during the use of such traditional agents.[15,16]

Inorganic nanoparticles encompass several NPs groups that can be defined according to their elemental composition. A complete and detailed list can be obtained from the Data and knowledge on Nanomaterials (DaNa)[17]. Pure elemental metallic NPs[18] (Au, Pt, Ag, Fe) are typically synthesized from their metal salt precursors. Due to well-known Localized Surface Plasmon Resonance (LSPR) characteristics, these NPs possess unique optoelectrical properties very useful in many areas as theragnosis or *in vivo* imaging.[19] Another group includes ceramics NPs[20] which are composed of a combination of covalent compounds, mostly oxides (e.g. CeO_2, SiO_2, TiO_2, ZnO). Although it is a heterogeneous group, they have some properties in common such as antibacterial activity, high heat resistance or chemical inertness. Among all the fields of application, biomedicals have been the most developed, considering ceramic NPs as excellent carriers of molecules (drugs, proteins, imaging agents) due to their high stability, high load capacity and the easily incorporation into hydrophobic and hydrophilic systems.[21] Finally, semiconductors NPs or QDs possess intermediate properties between metal and ceramic groups.[22] These nanosized luminescent crystals are made of combinations of elements found in groups II-VI, III-V or IV-VI of the Periodic Table (CdSe, ZnS, InP, GaN). The name of Quantum dots comes from the quantum confinement (or size) effects, occurring when the nanoparticle dimensions are reduced to few nanometers, that define their properties. For example, its optical properties are derived from the bandgap, which is the energy difference between the valence band to the conductance band. In this way, when an excited electron drops back into the valence band, it releases its energy by the emission of light, which depends on wide of this bandgap. The wavelength of the light emitted depends as much on the composition as on the shape and size. As a result, it is possible to engineer their optical properties by the variation of their size. Such distinct optoelectronic properties explain the success and increase application of QDs in bio-imaging, drug delivery, electronics and photovoltaics.[23]

Unlike their corresponding macroscale counterparts, the determination of the concentration and size distribution of colloidal nanocrystals is still an analytical challenge.[24] In the case of metallic NP, methodologies based on Ultraviolet-Visible (UV-Vis) spectroscopy have been developed to find out size, shape and even the Np size dispersion, based on the dependence they present with the maximum wavelength at

ARTICLE

the LSPR peak.[25] For example, the maximum absorbance in spherical AuNPs is between 505 and 580 (corresponding to sizes among 2 and 100nm);[26] while in the case of nanorods, the longitudinal LSPR mode is placed from 650 to 1000 nm.[27] UV-Vis spectroscopy can be also used to determine the particle number concentration of some typical QDs. However, since the extinction coefficient (ε) varies with the size of the NPs, the Beer–Lambert law cannot be used. In the specific case of CdTe, CdSe and CdS nanocrystals, the most accepted and recognized method is based on the procedure developed by Peng *et al*.[28] This assessment, made use of numerous data obtained by Transmission Electron Microscopy (TEM) and X-ray Diffraction (XRD) in a combination with theoretical approaches to obtain empirical curves that provides a simple and quick estimation of the concentration and size of the NPs. The derived equations are specific for CdTe, CdSe and CdS QDs, because the structure of the elemental cell in this NPs is always the same regardless of the size of the NP.

Probably, colloidal NPs sizing techniques most widely used today are dynamic light scattering (DLS) and nanoparticle tracking analysis (NTA). Both techniques operate on the principle of light scattering and provide information about average size, size distribution profiles and NPs aggregation by measuring fluctuations in the scattered light originated from both the Brownian motion of the NPs and from the constructive or destructive interferences of the scattered light from the neighbouring nanoparticles .[29] DLS measures the fluctuations in scattered light intensity, which are correlated to the particle hydrodynamic diameter via the correlation function and the Stokes–Einstein equation. However, due to Rayleigh theory, the intensity of scattered light is proportional to the sixth power of the diameter, and thus the analysis is heavily weighted towards larger particle size.[30] As a result, although a rapid and simple method, the presence of aggregates or dust can lead to underestimation or overestimation of results. Hence, its major application field is the characterization of samples with low-polydispersity index.

NTA is a high-resolution analysis technique that is able to distinguish small differences between two nanoparticles by tracking their individual nanoparticle movements within a solution, based on diffusion and Brownian motion or light scattering intensity. One key advantage of NTA is that information provided is not biased towards larger nanoparticles or aggregates.[31] The counting of individual particles also allows estimating the NPs concentration. Again, such measurements rely on light scattering measurements. Thus, accuracy of the estimated concentration values is low for nanoparticles with low refractive indices. Unfortunately, all these light scattering methodologies are not useful for characterization of fluorescent nanoparticles (e.g. QDs) as light emission from the NPs seriously affect the light dispersion measurements.

Interestingly an alternative method for inorganic nanomaterial characterization is the so-called Single-Particle Inductively Coupled Plasma Mass Spectrometry (spICP-MS). sp-ICPMS can be considered today as a key analytical technique in assessing the fate, behaviour, and distribution of inorganic ENMs in various sample matrices. It can be used to quantify the difference between ionic and particulate signals, measure the nanoparticle concentration (particles per volume), and determine the particle size and size distribution in aqueous colloidal nanoparticle suspension. In addition, it enables users to investigate particle agglomeration and dissolution. In order to apply spICP-MS, a very diluted sample containing nanoparticles is introduced in the ICP-MS instrument with fast mass scanning speed capacity. Under those conditions, only one nanoparticle at a time enters the plasma, producing a high intensity individual event that the instrument can distinguish from the continuous background signal. The number of observed pulses at the detector is related to the nanoparticle concentration by the nebulization efficiency and the total number of nanoparticles in the sample, while the size of the nanoparticle is related to the pulse intensity. Obviously, the lower the dwell time, the higher the scan speed and in turn the higher the capacity to discriminate between events (i.e. individual NPs). In this context, state-of-the-art ICP-MS instruments enable to operate with dwell times in the order of few microseconds (ranging from 0.1 to 10 μs). However, such requisites bring with them limitations on the NP detection limits. In this regard, the minimum detectable NP diameter with the conventional sp-ICPMS instruments is of about 10 nm for single-element homogeneous NPs. The potential of spICP-MS to assess the presence of different NP populations coexisting in a sample has been recently demonstrated by their detection in a Reference Material where it was thought that there was only one single type of nanoparticle. The presence of such different nanoparticle populations in the sample, that otherwise went unnoticed, were later corroborated using High-resolution scanning electron microscopy (HR-SEM). Such study highlighted the need to improve the characterization of NP Reference Materials using novel analytical approaches offering complementary advanced information.[32] . Although there are already a vast number of applications of spICP-MS for the analysis of different samples and different matrices,[33] many critical advances are expected in the near future such as: novel sample treatment procedures and nebulization systems to improve particle recovery rates and little to no species transformation, shorter detector dwell times, automated data reduction software or the online combinations with adequate separation techniques.[34]

Another critical issue in NP characterization is the detailed elemental characterization of hybrid core-shell NPs with multielemental cores and different shell layers specifically produced during the synthesis to provide: (i) protection against environmental changes or photo-oxidative degradation, (ii) increase luminescent quantum yields by passivating the surface trap states and (iii) create another route for optoelectronic modularity. Obviously, ICP-MS plays again a pivotal role in this task. In a pioneer attempt to use of ICP-MS for NPs characterization, it was showed that elemental stoichiometry of PbSe QDs was far from the expected theoretical 1:1 ratio.[35] A global excess of Pb was detected, which was confirmed with imaging and microscopy data. It was concluded that the NP was a composed of a quasi-

stoichiometric PbSe core covered with a Pb-enriched surface shell. Since then, there have been other proposals in which MS measurements have been complemented with data from other techniques to provide reliable elemental ratios.[36] Later on, isotope dilution was employed to determine accurately the elemental distribution of the core and shell of CdSe QDs along the synthesis.[37] In that way, it was proved that the Cd excess observed was due to the growth of a mixed shell of CdS/ZnS over the CdSe crystal core.

It is worth mentioning that, despite the supremacy of elemental mass spectrometry for these determinations, there are publications that use other methodologies as the combination of different X-ray spectroscopies with microscopy techniques for the same purpose. For example, the determination of the elemental composition of individual $Cu_2ZnSnSe_4$ NPs employing Energy-dispersive X-ray spectroscopy (EDX) with Transmission electron microscopy (TEM) and electron energy-loss spectrometry (EELS). The elemental analysis is obtained due to the excellent spatial resolution of this method.[38]

Obviously, bulk analysis does not provide information about the presence of different nanoparticle populations coexisting in the same sample. For that purpose, different separation techniques have been employed to discriminate the constituents of target mixtures of potential NP species based on differences in their chemical or physical properties (i.e. size, mass, density or chemical affinity). Such techniques must be coupled on-line to both molecular (UV-Vis, Fluorescence, DLS) or atomic (ICP-MS) detectors depending on the type of information sought. Among the different types of inorganic NPs, QDs have been profusely studied. For example, Pitkänen *et al.* proposed the online coupling of SEC to Quasielastic light scattering (SEC/QELS) for the size characterization of functionalized CdSeS/ZnS QDs.[39] The methods described so far determine the average size of a sample and its polydispersity index (PdI), but they do not indicate whether that size is due to the existence of a single population or several remarkable populations. If an adequate separation technique is used before the detector, the size of each of these remarkable populations and its contribution to the sample can be determined. As in this case, where the optical properties of the NMi rely largely on its size, it is very important to have a technique that allows describing each of the different populations present.

Alternatively, Menéndez-Miranda *et al.* [40] resorted to Asymmetric Flow Field-Flow Fractionation (AF4) coupled on line to fluorescence and ICP-MS to detect and characterize the diverse nanosized populations coexisting in the relatively complex mixtures obtained after the different synthesis routes and purification methods used during CdSe-ZnS QDs production. Elemental ratios could be accurately measured in the individually separated nanosized populations which enabled detection and identification of even the unexpected concomitant CdS nanosized species originated when ZnS shell was promoted directly in the same solution where the CdSe core was produced (one pot synthesis). Interestingly, the use of ICP-MS/MS in this case, opened the door to the sensitive

and free-of-interference measurement of highly interfered elements such as Se, Zn and especially P and S.

Therefore, the AF4-ICP-MS/MS approach was presented as a highly valuable diagnostic tool to control the quality and purity of the resulting NP solutions obtained.[40] Multi-Angle Light Scattering (MALS) has been also widely used as AF4 detector in many different applications, and particularly to identify the different nanosized populations present in a sample.[41] In this case, deconvolution of the AF4 peaks was critical to unveil the different aggregation states of QDs.[41] Furthermore, Meermann *et al*[42]. resorted to enriched isotopes to differentiate between natural and engineered nanoparticles by the combination of AF4 with sector-field ICP-MS. Iron oxide nanoparticles isotopically enriched in ^{57}Fe coated with a SiO_2 shell ($^{57}Fe@SiO_2$ ENPs) were used in this matter.

3. Surface modification

Most of the synthesis routes that are used to obtain inorganic NPs are carried out in organic media, since they are more efficient and provide a better control over the characteristics of the final products. Therefore, when intended to be applied in biomedical applications, it is mandatory a surface functionalization to render NPs with stability in biological buffers and adequate biocompatibility. Of course, the whole process should be conducted while maintaining the original advantageous optoelectronic properties of the NPs.[43]

However, any change in the NP surface's environment or in the composition of the solvent often brings with variation of some characteristics of the NPs, as occurs with their optical properties and colloidal stability. Once again, diagnostic tools are required to detect and quantify the success on the functionalization and to control such eventual changes on the ENPs properties prior to their subsequent use. For example, the Surface plasmon resonance (SPR) peak is strongly influenced by the refractive index at the adjacent surface interface of the nanoparticle, and this is highly affected by adsorptions of materials onto the surface of metal nanoparticles (i.e. biofuncionalization or binding interactions).[44] Actually, SPR is the basis of many standard tools for measuring interactions between NPs with biomolecules. [45]

Before carrying out nanoparticle surface modifications, it is essential to know the type of ligand that best suits with the subsequent application of the NPs. For this purpose, according to Heuer-Jungemann *et al*.,[46] there are many important parameters to consider such as the chemical composition of the NP surface, the target environment where the particles are going to be released, the desired NP morphology and the need for possible further chemical modifications of the ligand shell.

One of the most widespread and effective strategies for surface modification is the exchange of ligands mainly due to its simplicity. It consists of the replacement of the hydrophobic coordinating agents that originally cover the NPs in organic media with bifunctional molecules. These molecules have a functional group at one of their ends that binds directly to NP's surface and a polar group at the other end that provides them
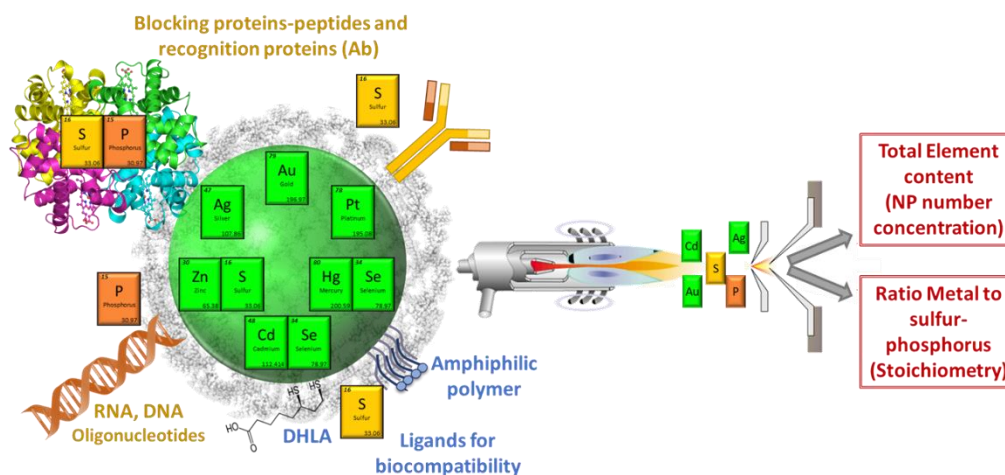
Figure 2. Schematics of the key role of ICP-MS/MS in NMi characterization. Potential different elements detected and their origin are indicated.

with water solubility while preventing their aggregation. Bidentate thiolated ligands, such as dihydrolipoic acid (DHLA), are one of the most commonly used.[47] Here, characterization of the surface coverage of ligands on the colloidal inorganic nanoparticles is an issue of paramount importance as this value can determine macrophage–nanoparticle interactions, protein corona formation, and cellular nanoparticle uptake. In addition, biosensing applications require nanoparticles that are very stable in biological samples, and to minimize unspecific adsorptions, both issues are closely related to the nanoparticle surface ligand density.[48] There are several strategies that assess the number of ligand molecules covering the surface of colloidal inorganic NPs (surface ligand density) and in most of them it is made clear the need for integrated platforms to characterize this transformation.[49,50] In this context, Garcia-Cortes et al.,[51] resorted to the combination of information provided by XRD, electron microscopy and ICP-MS to unveil the local structure of ions within a novel QD nanostructure, the number of atoms constituting the QDs core and the NP number concentration in a colloidal solution. Later on, the use of the AF4-ICP-MS/MS platform allowed the accurate and precise determination of the metal to sulfur ratio in the isolated target functionalized nanoparticle species. In this regard, because most of ligands conventionally employed to modify the NP surface contain S in its structure (e.g. DHLA), the S detected can be related to the ligand density. Figure 2 shows the source of some of the elements measured by ICP-MS present in the inorganic NPs, being able to arise two cases for the S quantification. In the simplest case, the NP does not have sulphur in its structure and thus the ligand density is given directly from the S/Metal ratio, as it is the case of HgSe NPs surface modified with DHLA.[49] Alternatively, if the NP has already S in its structure, as it happens with ZnS[51] or CdSe/ZnS QDs,[52] the ligand density value can be obtained from the increase of the S/Metal ratio after surface modification with the S-containing ligand. It is important to highlight here the paramount importance of the sensitive S detection in all these novel approaches (see Figure 2). In this context, the new ICP-MS/MS instrument released in 2012 played a critical role.[53]

The high selectivity offered by the MS/MS configuration reduced chemical noise and background significantly allowing a virtually interference-free detection of P and S as PO^+ and SO^+. This resulted in a significant improvement in their detection limits in comparison to previous ICP-MS configurations.

Another widely used strategy for surface modification is based on the use of amphiphilic polymers. These compounds have several hydrophobic chains with a hydrophilic end. The hydrophobic chains cross over the NP surface chains, leaving the hydrophilic end remains on the outer end giving aqueous stability to the entire structure.[54] The most commonly used are the polyethylene glycol (PEG) chains and the polymers based on maleic anhydride in combination with primary amines.[55] Given the size of the polymer chains, this strategy implies a greater variation in the nanostructure size than in the case of ligand exchange. Once again different techniques have been employed so far to assess ligand density. A nearly general model for quantitative characterization of such organic layer and core-shell NPs were developed Torelli et al. [56] employing X-ray photoelectron spectroscopy (XPS) and resorting to different computational approaches that mitigated the electron attenuation length. Another remarkable example is that of Sebby et al., who used microscale thermogravimetric analysis (μ-TGA) to quantify the NP-linked polymer.[57] They concluded that TGA is a convenient technique for the quantification of ligands bound to inorganic NPs while sacrificing a minimal amount of sample.

It is worth mentioning the work of Bouzas et al.[52] comparing the solubilization of CdSe/ZnS core-shell QDs using both approaches, amphiphilic polymer and ligand exchange with DHLA. Resulting nanoscale water stable products obtained were assessed resorting again to the AF4 coupling to ICP-MS/MS. Molecular detectors such as UV-Vis and fluorescence were also online integrated in the analytical platform. This approach allowed to reveal that ligand exchange solubilisation procedure with DHLA removed completely the eventual side nanoparticulated populations of CdS generated during one-pot synthesis of CdSe-ZnS QDs, which can ruin the subsequent final

bioapplication. On the contrary, as mentioned above, removal those impurities species from the solubilization using amphiphilic polymers, would require a multiple-step (2-pot) synthesis or further purification.

4. Bioconjugation analysis

In order to make inorganic NPs useful in the challenges currently faced in bioanalysis, it is mandatory to make them biocompatible and specific to the desired target. For such purpose, it is required to perform an adequate NPs functionalization with appropriate biomolecules providing the desired selectivity and recognition capabilities. Again, knowledge on the surface chemistry of the resulting bioconjugated NPs is required to ensure the improved biocompatibility, sensitivity, and specificity features, providing the grounds for the multitude of applications in biosensing, biolabeling, and delivery of therapeutic agents. Thus, the bioconjugation of NPs to specific biomolecules such as DNA, aptamers, enzymes or antibodies, constitutes one of the most active fields of research in nanoscience today. Interestingly, most of these biomolecules contain ICP-detectable elements such as P and mostly, S (see Figure 2). However, this growing interest has not led to significant progress on the new procedures for purification and characterization of the bioconjugates. In fact, in addition to parameters to be controlled after surface transformation such as elemental ratio, ligand density, NP purity and assessment of side NP populations or size, it is also necessary in this case to determine the bioconjugation reaction efficiency. Therefore, it is critical to have analytical methodologies able to provide the accurate quantitative characterization of the surface coverage of NPs with specific biomolecules, in order to evaluate the success and reproducibility of the corresponding conjugation reactions thereby facilitating the design and development of reliable quantitative bioassays.[58,59]

Common strategies for the purification and characterization of bioconjugates usually make use of physical processes as dialysis, centrifugation in several cycles, ultrafiltration, re-dispersion and ultracentrifugation.[60,61] However, these methodologies are limited by their low efficiency and separation resolution. Commercial membranes have restricted pore sizes as well, limiting again the efficiency on the isolation of the desired bioconjugation species. Adequate characterization of the bioconjugation process can be approached from different perspectives depending on the way in which the measurements are carried out.

4.1. Indirect methods

Reaction efficiency and stoichiometry of the resulting bioconjugates can be obtained from independent analysis of its individual components, NPs and biomolecules.

In the most common approach biomolecules attached to the NPs are assumed to be those determined by difference taking into account the corresponding excesses that are present in the washing or discarded solutions. Due to the mainly protein nature of biomolecules, these are determined by the conventional methods employed in biotechnology for protein content quantification (Lowry assay, Bradford assay or ELISA kits)[62] or based in fluorescence measurements of labelled proteins.[63] However, often these methods suffer of a reduced specificity. Moreover, as the biomolecules are generally determined after several washing steps, recoveries are sometimes very low. Along these washing stages, biomolecules can be lost, or part of the adsorbed proteins that block the surface of the NPs can be detached during the process, leading to inaccurate results.

In another approach the resulting bioconjugate is thoroughly purified first and then break down into its individual components to be measured independently. For example, Liu *et al.*[64] proposed a generic protein-NPs conjugation characterization method based in the chemical digestion of the bioconjugated proteins into their constituent amino acids that are then released to the solution to be quantified by HPLC-FLD.Either way, the concentration of NP, and in turn the stoichiometry of the reaction, are obtained after their acid digestion and measure the solutions by mass spectrometry.[65]

Indirect methods have some clear disadvantages as the potential error likely associated to the eventual low analyte recoveries and/or possible nanoparticle alterations occurring along the different number of steps required along the procedure. Furthermore, they only provide an average NP:biomolecule ratio in the resulting bioconjugate without any information about the interaction between components or the presence of potential different bioconjugate populations with different stoichiometry NP to biomolecule.

4.2. Direct methods

The most appropriate strategies to characterize bioconjugation involve the direct analysis of the bioconjugate as a whole. Sought information (reaction efficiency, global NP:biomolecule stoichiometry and assessment of individual bioconjugate populations with corresponding stoichiometries) can be obtained from the direct analysis of the resulting bioconjugate solutions. This implies that bioconjugations are analysed as indivisible entities. A clear advantage against indirect methods is the amount of material needed that, although it depends upon instrument sensitivity, is significantly lower than that of standard methods for protein quantification. These methods can be divided into two categories according to when the purification is performed, before or during the analysis.

As mentioned before, determination of metal to sulfur ratios by ICP-MS has established as a promising alternative to estimate the NP:biomolecule stoichiometry directly in bioconjugate. In this regard, determination of bulk metal to sulfur ratios has been already reported for the quantification of the average protein corona content in gold NPs.[66,67] However, S is often present not only in the biomolecule but also in the core or shell of the NPs (e.g., ZnS, AgS, CdS),[52] or has been already incorporated during surface functionalization in the form of S-containing ligands (see previous section and Figure 2), thereby making the use of ICP-MS more difficult.

Unfortunately, such direct ICP-MS-based strategies, although very useful for assessing interactions between NPs with S-containing biomolecules, provide exclusively the average ratio of the molecules (e.g., ligands, proteins, etc.) attached to the NP. Additionally, there is no way to ensure that each and every individual component present in the solution are in fact linked forming part of a bioconjugate entity.

A definitive step forward is the use of a separation/fractionation technique in order to isolate the likely still present traces of free components from the bioconjugate species and, at best, the individual bioconjugate populations with different stoichiometries. Nonetheless, the resolution power strongly depends on the molecular weight and the isoelectric point of the biomolecules attached to the NPs. The main separation techniques used so far are detailed below.

Electrophoretic techniques are based on the motion of dispersed charged particles under the influence of a spatially uniform electric field. The most employed techniques for NPs analysis are Gel Electrophoresis (GE) and Capillary Electrophoresis (CE). Separation of bioconjugates by GE is possible if the biomolecule bound to a NP changes significantly its overall effective size or charge. If so, bioconjugates with different ratios can be separated based on their differential electrophoretic mobility. However, quantification after the gel separation is difficult and is commonly carried out off line by removing and extracting the desired bands prior to the analysis.[68] Furthermore, this approach is limited by the strong interaction of the different functional groups over the NP surface with the gel sieving. Resolution power is limited as well. Finally, not all NP–biomolecule conjugates are amenable to be separated using this strategy.[58] The separation of NPs and bioconjugates can also be done using CE based upon their charge-to-size ratio. For example Pereira *et al.*[69] built developed a Capillary electrophoresis system coupled to Laser-induced Fluorescence (LIF) for the characterization of commercial QDs and their bioconjugates. They also proved the different techniques of bioconjugation (non-selective and selective). Although biomolecules have many functional groups that increase net charge and therefore separation, they also promote uncontrolled polymerization. This implies that the different bioconjugates have similar migration times and therefore, the difference between them is lower. However, this methodology is very successful for the development of diffusion immunoassays as the resulting longer migration time for the immunoconjugate suggests a further increase in the immunoconjugate's net-negative charge.

Among the wide variety of chromatographic modes available, Size Exclusion (SEC) and Hydrodynamic chromatography (HDC) are the most commonly used for NMi analysis. In particular, SEC has been typically used in the determination of the bioconjugate stoichiometry.[70] In fact, resolution power in SEC is generally superior to that in AF4, however, it presents irreversible interactions of the NMi with the stationary phase that is damaged unless it is modified by blocking the packing. Such uncontrolled interactions negatively affect NP surface (i.e. polymer over the NP can be partially lost) and bioconjugate recovery from the column as demonstrated by

Trapiella *et al.* during analysis of CdSe/ZnS QDs and their bioconjugates using SEC with online molecular and elemental integrated detection.[71] On the one hand, elemental detector provided information about the elemental ratios and recovery while fluorescence was used to prove the degradation of the QDs, by checking the emission of the free detached polymer. This platform revealed the importance of the inorganic shell for the adequate and stable polymer coating attachment and consequently, for the successful subsequent bioconjugation.

Finally, Field flow fractionation is without a doubt the most widely used technique for the separation of nanoparticles and their bioconjugates.[72,73] In this regard, Menendez-Miranda *et al*. were able to determine the conjugation effectiveness between a model antibody (Ab) and CdSe/ZnS core-shell QDs, surface-coated with an amphiphilic polymer using AF4-ICP-MS.[14] Due to the fact that elemental signal provided by ICP-MS is mostly species independent, the efficiency of the bioconjugation could be obtained by the ratio between the areas of the resolved peaks from the bioconjugate species and the free QDs. Interestingly, this feature also allowed to evaluate the possible losses due to undesired interactions between the QDs or their bioconjugates with the permeation membrane or other wetted surfaces in the channel (i.e. recovery) by injecting samples, with and without applying cross-flow, and comparing the resulting Cd and Se peak areas. Notably composition and pH of the carrier was found to be critical parameters to ensure and efficient separation while ensuring high species recovery from the AF4 channel (> 95%).

Later on Bouzas *et al.*, used the same platform to achieve for the first time the determination of such ratios directly in conjugate mixtures of CdSe/ZnS core–shell QDs with monoclonal Antibodies (QD:Ab) in a single run without any previous sample preparation.[74] Two independent quantitative strategies were developed. The first one provided the global (average) QD:Ab ratio and was based on the measurement of Cd to S area ratios in the AF4 peaks obtained for pure and isolated bioconjugated QDs, which were then translated into the corresponding Cd to S molar ratios using external flow injection (FI) calibration. As the number of Cd and S atoms per QD was experimentally obtained previously and the number of S atoms per mole of antibody was known beforehand such Cd to S molar ratio determined in the bioconjugate peak could be easily translated into the sought global QD:Ab ratio.

The second strategy allowed to go beyond disclosing the mixture of the different species with different QD:Ab ratios eventually present in the bioconjugated sample. In this case, the Cd:S intensity ratio was point-by-point determined along the bioconjugate peak obtained. Notably such elemental ratio changed significantly along its central part because of the continuous elution of unresolved bioconjugated species with increasing QD:Ab ratios while it was stable in the two regions at the beginning and end of the bioconjugate peak that were ascribed to the parts of the limit populations with the lowest and highest QD:Ab ratios eluting singly from the AF4. Intensity ratios in such two limit bioconjugate populations were translated into Cd:S molar ratios using again external FI calibration. Such molar ratios were in turn used to obtain the

individual QD:Ab ratios for the lower and upper limit populations. Furthermore, their individual relative abundances within the bioconjugate mixture could be estimated as well using the mathematical treatment shown in Figure 3. One of the most striking conclusions of the work was the wide range of stoichiometries that could be detected ranging from 4 Ab per each QD to 5 QD per each Ab depending on the molar ratios assayed during the reaction.
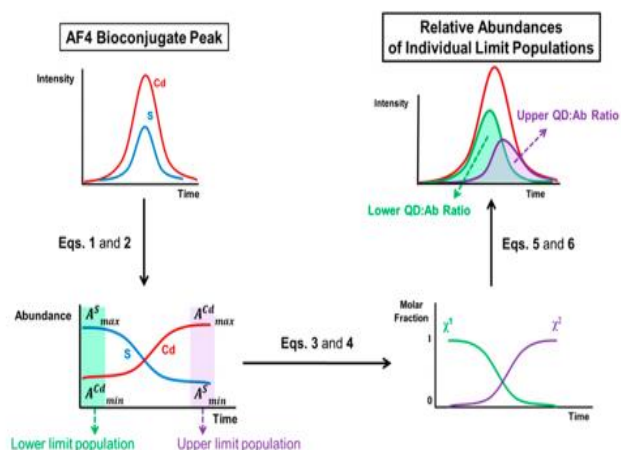

Figure 3. Schematic representation of the AF4-ICP-MS/MS procedure designed to calculate relative abundances of mixtures of bioconjugates with different QD:Ab ratios using Cd:S intensity ratio measurements point-by-point determined along the bioconjugate peak. Reprinted from Bouzas et al.[74], copyright 2019, with permission from the American Chemical Society.

The approach proposed was general as can be applied to any type of inorganic NP (independently that it contains previously sulfur in the core, shell, or in the ligands attached), while it is linked to sulfur-containing biomolecules. Of course, the only requisite to meet is that the conjugation of the S-containing biomolecules to the NP must result in a change in the S:Cd ratio that could be measured by ICP-MS/MS. Interestingly the approach is neither constrained by the type of interaction, which may be either chemical (bioconjugation) or physical (protein corona). However, there are also limitations as the need to isolate the bioconjugate peak from that of NPs itself (excess of free NPs). Information provided about the individual populations present is partially limited as well, since it is assumed that only two limit populations are present in the mixture. Additionally, the stoichiometry information obtained for the different bioconjugate populations could be well complemented with their hydrodynamic actual size provided by light scattering-based techniques such as DLS or MALS.[41]

4.3. Protein corona

It is worth mentioning here that once the NPs, free or as part of bioconjugates, are transferred to a biological media, a superior structure called protein corona is potentially formed. A shell of naturally present biomolecules, mainly proteins but also other biomolecules such as lipids and sugars, can surround the nanoassembly. These biomolecules are not chemically linked to the NPs as explained before for bioconjugation but are adsorbed on the surface.[75] Obviously,

this new surface modification can vary the physicochemical properties of NPs as well, by increasing their size or promoting their aggregation.[76] Nevertheless, this process is of tremendous importance as it determines completely the reactivity of the NMi in the different media.[77]

Some studies focused on the use of complementary physical and spectroscopic methods to study interaction of proteins with ENMs. As an example, conjugation of BSA with AuNPs has been quantitatively characterized by resorting to the use of DLS, AF4, ES-DMA, fluorescence spectrometry, and ATR-FTIR to obtain information regarding both molecular surface density and molecular conformation of BSA adsorbed onto AuNPs.[78]

As in the case of bioconjugates, there are many experimental direct and indirect approaches that can be employed for the characterization of protein corona.[79] The typical indirect method makes use of enzymatic digestion of the proteins adsorbed to the NP surface followed by the analysis by gel electrophoresis or mass spectrometry.[80] One possible alternative consists of the use of isotopically enriched sulfur (^{34}S) in the engineered nanoparticle structure. In that case, a simple sulfur isotope ratio measurement by ICP-MS allowed the assessment of NP:biomolecule stoichiometries.[81] Obviously, this procedure requires a previous synthesis of the nanoparticles incorporating the enriched S. On the other hand, Matczuk et al.[67] proposed capillary electrophoresis (CE) coupled to ICP-MS as a direct approach to determine the stoichiometric composition of the protein corona of AuNPs. Following a procedure similar to that explained previously, they related S and Au content determined by ICP-MS to total protein and AuNP content, respectively.

5. Conclusions

Analytical methodologies offering complementary information aiming at providing an extensive inorganic ENPs knowledge are certainly necessary to get a better understanding of the NPs behaviour and characteristics. A comprehensive characterization of ENPs will offer on the one hand a solid basis for the design of nanomaterials with enhanced properties of high added value in bioanalytical applications. On the other hand, it will facilitate the production of safer nanomaterials (i.e. minimizing environmental risks associated to their size, morphology, or composition).

An ideal characterization method should be capable of providing information about size and shape of the ENPs, purity, number concentration, elemental composition or surface ligand coverage, among other key parameters. Clearly such universal characterization method has not yet been developed. In fact, depending on both the native properties of the NPs and the environment, the characterization techniques have to be selected on a case-by-case basis. Among the different options available, the coupling of a NP separation technique on line to molecular (e.g. VIS-UV, fluorescence), light scattering and ICP-MS detection techniques is expected to be established in the near future as an excellent choice for the assessment of inorganic NMi synthesis, functionalization and bioconjugation for their eventual use in reliable

quantitative bioassays. Additionally, it allows the assessment of the effectiveness (and stoichiometry) of the bioconjugations of NPs to biomolecules, another important aspect rarely tackled so far. Such integrated platforms have the potential to be slowly considered as routine tools for comprehensive functionalized inorganic NPs characterizations.

Last but not least, depending of the analytical technique selected for detection, special care should be taken when preparing the sample containing the NPs. This is a critical parameter that merits special consideration as NPs are characterized by an extremely high reactivity due to their high surface to volume ratio. Therefore, there is a high risk of eventual aggregations and surface perturbations during sample preparation and analysis. This is a critical requirement for benefiting from the impressive capabilities of the powerful instrumental detection platforms described in this review.

Conflicts of interest

Acknowledgements

Notes and references

1   M. C. Roco, in *Nanotechnology Commercialization*, John Wiley & Sons, Inc., Hoboken, NJ, USA, 2017, pp. 1–23.
2   M. Knell, in *Nanotechnology and the Challenges of Equity, Equality and Development*, eds. Cozzens Susan E. and J. and Wetmore, Springer Netherlands, Dordrecht, 2010, pp. 127–143.
3   O. J. of the E. Union, *Commission recommendation of 18 October 2011 on the definition of nanomaterial*, 2011, vol. 2011/696/E.
4   J. Jiang, G. Oberdörster, A. Elder, R. Gelein, P. Mercer and P. Biswas, *Nanotoxicology*, 2008, **2**, 33–42.
5   A. Albanese, P. S. Tang and W. C. W. Chan, *Annu. Rev. Biomed. Eng.*, 2012, **14**, 1–16.
6   D. R. Baer, M. H. Engelhard, G. E. Johnson, J. Laskin, J. Lai, K. Mueller, P. Munusamy, S. Thevuthasan, H. Wang, N. Washton, A. Elder, B. L. Baisch, A. Karakoti, S. V. N. T. Kuchibhatla and D. Moon, *J. Vac. Sci. Technol. A Vacuum, Surfaces, Film.*, 2013, **31**, 050820.
7   G. T. Hermanson, ed. G. T. B. T.-B. T. (Third E. Hermanson, Academic Press, Boston, 2013, pp. 1–125.
8   L. Arms, D. W. Smith, J. Flynn, W. Palmer, A. Martin, A. Woldu and S. Hua, *Front. Pharmacol.*, 2018, **9**, 802.
9   A. Nel, *Science (80-.).*, 2006, **311**, 622–627.
10 F. Caputo, J. Clogston, L. Calzolai, M. Rösslein and A. Prina-Mello, *J. Control. Release*, 2019, **299**, 31–43.
11 F. Laborda, E. Bolea, G. Cepriá, M. T. Gómez, M. S. Jiménez, J. Pérez-Arantegui and J. R. Castillo, *Anal. Chim. Acta*, 2016, 904, 10–32.
12 S. Mourdikoudis, R. M. Pallares and N. T. K. Thanh, *Nanoscale*, 2018, **10**, 12871–12934.
13 K. Tiede, A. B. A. Boxall, S. P. Tear, J. Lewis, H. David and M. Hassellöv, *Food Addit. Contam. Part A*, 2008, **25**, 795–821.
14 M. Menéndez-Miranda, J. R. Encinar, J. M. Costa-Fernández and A. Sanz-Medel, *J. Chromatogr. A*, 2015, **1422**, 247–252.
15 S. K. Nune, P. Gunda, P. K. Thallapally, Y.-Y. Lin, M. Laird Forrest and C. J. Berkland, *Expert Opin. Drug Deliv.*, 2009, **6**, 1175–1194.
16 N. Naseri, E. Ajorlou, F. Asghari and Y. Pilehvar-Soltanahmadi, *Artif. Cells, Nanomedicine, Biotechnol.*, 2018, **46**, 1111–1121.
17 DaNa, https://www.nanopartikel.info/en/.
18 V. Mody, R. Siwale, A. Singh and H. Mody, *J. Pharm. Bioallied Sci.*, 2010, **2**, 282.
19 R. Singla, A. Guliani, A. Kumari and S. K. Yadav, in *Nanoscale Materials in Targeted Drug Delivery, Theragnosis and Tissue Regeneration*, ed. S. K. Yadav, Springer Singapore, Singapore, 2016, pp. 41–80.
20 S. Thomas, B. S. P. Harshita, P. Mishra and S. Talegaonkar, *Curr. Pharm. Des.*, 2015, **21**, 6165–6188.
21 A.-I. Moreno-Vega, T. Gómez-Quintero, R.-E. Nuñez-Anita, L.-S. Acosta-Torres and V. Castaño, *J. Nanotechnol.*, 2012, **2012**, 1–10.
22 V. Biju, T. Itoh, A. Anas, A. Sujith and M. Ishikawa, *Anal. Bioanal. Chem.*, 2008, **391**, 2469–2495.
23 L. Cui, C. Li, B. Tang and C. Zhang, *Analyst*, 2018, **143**, 2469–2478.
24 L. Trapiella-Alfonso, M. Menéndez-Miranda, J. M. Costa-Fernández, R. Pereiro and A. Sanz-Medel, *Mater. Res. Express*, 2014, **1**, 015039.
25 S. Eustis and M. A. El-Sayed, *Chem. Soc. Rev.*, 2006, **35**, 209–217.
26 S. Link and M. A. El-Sayed, *Int. Rev. Phys. Chem.*, 2000, **19**, 409–453.
27 A. Lapresta-Fernández, A. Salinas-Castillo, S. Anderson de la Llana, J. M. Costa-Fernández, S. Domínguez-Meister, R. Cecchini, L. F. Capitán-Vallvey, M. C. Moreno-Bondi, M.-P. Marco, J. C. Sánchez-López and I. S. Anderson, *Crit. Rev. Solid State Mater. Sci.*, 2014, **39**, 423–458.
28 W. W. Yu, L. Qu, W. Guo and X. Peng, *Chem. Mater.*, 2004, **16**, 560–560.
29 C. M. Maguire, M. Rösslein, P. Wick and A. Prina-Mello, *Sci. Technol. Adv. Mater.*, 2018, **19**, 732—745.
30 B. J. Frisken, *Appl. Opt.*, 2001, **40**, 4087–4091.
31 V. Filipe, A. Hawe and W. Jiskoot, *Pharm. Res.*, 2010, **27**, 796–810.
32 A. R. Montoro Bustos, K. P. Purushotham, A. Possolo, N. Farkas, A. E. Vladár, K. E. Murphy and M. R. Winchester, *Anal. Chem.*, 2018, **90**, 14376–14386.
33 D. Mozhayeva and C. Engelhard, *J. Anal. At. Spectrom.*, , DOI:10.1039/C9JA00206E.
34 D. Mozhayeva and C. Engelhard, *J. Anal. At. Spectrom.*, 2020.
35 I. Moreels, K. Lambert, D. De Muynck, F. Vanhaecke, D.

Poelman, J. C. Martins, G. Allan and Z. Hens, *Chem. Mater.*, 2007, **19**, 6101–6106.

36 E. Sotelo-González, L. Roces, S. García-Granda, M. T. Fernández-Argüelles, J. Costa-Fernandez and A. Sanz-Medel, *Nanoscale*, , DOI:10.1039/c3nr02422a.

37 A. R. Montoro Bustos, J. R. Encinar, M. T. Fernández-Argüelles, J. M. Costa-Fernández and A. Sanz-Medel, *Chem. Commun.*, 2009, 3107–3109.

38 W. Haas, T. Rath, A. Pein, J. Rattenberger, G. Trimmel and F. Hofer, *Chem. Commun.*, 2011, **47**, 2050–2052.

39 L. Pitkänen and A. M. Striegel, *Anal. Bioanal. Chem.*, 2016, **408**, 4003–4010.

40 M. Menéndez-Miranda, M. T. Fernández-Argüelles, J. M. Costa-Fernández, J. R. Encinar and A. Sanz-Medel, *Anal. Chim. Acta*, 2014, **839**, 8–13.

41 S. Faucher, G. Charron, E. Lützen, P. Le Coustumer, D. Schaumlöffel, Y. Sivry and G. Lespes, *Anal. Chim. Acta*, 2018, **1028**, 104–112.

42 B. Meermann, K. Wichmann, F. Lauer, F. Vanhaecke and T. A. Ternes, *J. Anal. At. Spectrom.*, 2016, **31**, 890–901.

43 L. Guerrini, R. A. Alvarez-Puebla and N. Pazos-Perez, *Mater. (Basel, Switzerland)*, 2018, **11**, 1154.

44 I. Mannelli and M.-P. Marco, *Anal. Bioanal. Chem.*, 2010, **398**, 2451–2469.

45 K. G. A.-S. Shevchenko Konstantin G. A4 - Cherkasov, Vladimir R. A4 - Tregubov, Andrey A. A4 - Nikitin, Petr I. A4 - Nikitin, Maxim P., *Biosens. Bioelectron.*, 2017, **v. 88**, 6-8–2017 v.88.

46 A. Heuer-Jungemann, N. Feliu, I. Bakaimi, M. Hamaly, A. Alkilany, I. Chakraborty, A. Masood, M. F. Casula, A. Kostopoulou, E. Oh, K. Susumu, M. H. Stewart, I. L. Medintz, E. Stratakis, W. J. Parak and A. G. Kanaras, *Chem. Rev.*, 2019, **119**, 4819–4880.

47 H. Takeuchi, B. Omogo and C. D. Heyes, *Nano Lett.*, 2013, **13**, 4746–4752.

48 P. S. Tang, S. Sathiamoorthy, L. C. Lustig, R. Ponzielli, I. Inamoto, L. Z. Penn, J. A. Shin and W. C. W. Chan, *Small*, 2014, **10**, 4182–4192.

49 D. Bouzas-Ramos, M. Menéndez-Miranda, J. M. Costa-Fernández, J. R. Encinar and A. Sanz-Medel, *RSC Adv.*, 2016, **6**, 19964–19972.

50 S. Roux, B. Garcia, J.-L. Bridot, M. Salomé, C. Marquette, L. Lemelle, P. Gillet, L. Blum, P. Perriat and O. Tillement, *Langmuir*, 2005, **21**, 2526–2536.

51 M. Garcia-Cortes, E. Sotelo-González, M. T. Fernández-Argüelles, J. R. Encinar, J. M. Costa-Fernández and A. Sanz-Medel, *Langmuir*, 2017, **33**, 6333–6341.

52 D. Bouzas-Ramos, M. García-Cortes, A. Sanz-Medel, J. R. Encinar and J. M. Costa-Fernández, *J. Chromatogr. A*, 2017, **1519**, 156–161.

53 S. D. Fernández, N. Sugishama, J. R. Encinar and A. Sanz-Medel, *Anal. Chem.*, 2012, **84**, 5851–5857.

54 R. B. Grubbs, *Polym. Rev.*, 2007, **47**, 197–215.

55 M. T. Fernández-Argüelles, A. Yakovlev, R. A. Sperling, C. Luccardini, S. Gaillard, A. Sanz Medel, J.-M. Mallet, J.-C. Brochon, A. Feltz, M. Oheim and W. J. Parak, *Nano Lett.*, 2007, **7**, 2613–2617.

56 M. D. Torelli, R. A. Putans, Y. Tan, S. E. Lohse, C. J. Murphy and R. J. Hamers, *ACS Appl. Mater. Interfaces*, 2015, **7**, 1720–1725.

57 K. B. Sebby and E. Mansfield, *Anal. Bioanal. Chem.*, 2015, **407**, 2913–2922.

58 K. E. Sapsford, K. M. Tyner, B. J. Dair, J. R. Deschamps and I. L. Medintz, *Anal. Chem.*, 2011, **83**, 4453–4488.

59 R. T. Busch, F. Karim, J. Weis, Y. Sun, C. Zhao and E. S. Vasquez, *ACS omega*, 2019, **4**, 15269–15279.

60 E. E. Lees, M. J. Gunzburg, T.-L. Nguyen, G. J. Howlett, J. Rothacker, E. C. Nice, A. H. A. Clayton and P. Mulvaney, *Nano Lett.*, 2008, **8**, 2883–2890.

61 N. Alele, R. Streubel, L. Gamrad, S. Barcikowski and M. Ulbricht, *Sep. Purif. Technol.*, 2016, **157**, 120–130.

62 C. D. Walkey, J. B. Olsen, H. Guo, A. Emili and W. C. W. Chan, *J. Am. Chem. Soc.*, 2012, **134**, 2139–2147.

63 S. L. Filbrun and J. D. Driskell, *Analyst*, 2016, **141**, 3851–3857.

64 N. A. Schneck, K. W. Phinney, S. B. Lee and M. S. Lowenthal, *Anal. Bioanal. Chem.*, 2016, **408**, 8325–8332.

65 A. R. Montoro Bustos, L. Trapiella-Alfonso, J. R. Encinar, J. M. Costa-Fernández, R. Pereiro and A. Sanz-Medel, *Biosens. Bioelectron.*, 2012, **33**, 165–171.

66 N. Fernández-Iglesias and J. Bettmer, *Nanoscale*, 2015, **7**, 14324–14331.

67 M. Matczuk, J. Legat, S. N. Shtykov, M. Jarosz and A. R. Timerbaev, *Electrophoresis*, 2016, **37**, 2257–2259.

68 F. Song and W. C. W. Chan, *Nanotechnology*, 2011, **22**, 494006.

69 M. Pereira and E. P. C. Lai, *J. Nanobiotechnology*, 2008, **6**, 10.

70 S. Süß, C. Metzger, C. Damm, D. Segets and W. Peukert, *Powder Technol.*, 2018, **339**, 264–272.

71 L. Trapiella-Alfonso, A. R. Montoro Bustos, J. R. Encinar, J. M. Costa-Fernández, R. Pereiro and A. Sanz-Medel, *Nanoscale*, 2011, **3**, 954.

72 H. S. Ferreira, B. Moreira-Alvarez, A. R. Montoro Bustos, J. R. Encinar, J. M. Costa-Fernández and A. Sanz-Medel, *Talanta*, 2020, **206**, 120228.

73 T. Rameshwar, S. Samal, S. Lee, S. Kim, J. Cho and I. S. Kim, *J. Nanosci. Nanotechnol.*, 2006, **6**, 2461–2467.

74 D. Bouzas-Ramos, J. I. García-Alonso, J. M. Costa-Fernández and J. Ruiz Encinar, *Anal. Chem.*, 2019, **91**, 3567–3574.

75 M. P. Monopoli, A. S. Pitek, I. Lynch and K. A. Dawson, in *Nanomaterial Interfaces in Biology: Methods and Protocols*, eds. P. Bergese and K. Hamad-Schifferli, Humana Press, Totowa, NJ, 2013, pp. 137–155.

76 L. Treuel, S. Brandholt, P. Maffre, S. Wiegele, L. Shang and G. U. Nienhaus, *ACS Nano*, 2014, **8**, 503–513.

77 V. H. Nguyen and B.-J. Lee, *Int. J. Nanomedicine*, 2017, **12**, 3137–3151.

78 D.-H. Tsai, F. W. DelRio, A. M. Keene, K. M. Tyner, R. I. MacCuspie, T. J. Cho, M. R. Zachariah and V. A. Hackley, *Langmuir*, 2011, **27**, 2464–2477.

79 C. Carrillo-Carrion, M. Carril and W. J. Parak, *Curr. Opin. Biotechnol.*, 2017, **46**, 106–113.

80 D. Docter, U. Distler, W. Storck, J. Kuharev, D. Wünsch, A. Hahlbrock, S. K. Knauer, S. Tenzer and R. H. Stauber, *Nat. Protoc.*, 2014, **9**, 2030–2044.

81 M. Menéndez-Miranda, D. Presa-Soto, A. Presa-Soto, J. M. Costa-Fernández and J. R. Encinar, *Spectrochim. Acta Part B At. Spectrosc.*, 2018, **149**, 99–106.